

Extracting the physical sector of quantum states

D Mogilevtsev^{1,2}, Y S Teo³, J Řeháček⁴, Z Hradil⁴, J Tiedau⁵,
R Kruse⁵, G Harder⁵, C Silberhorn^{5,6}, L L Sanchez-Soto^{5,6}

¹ Centro de Ciências Naturais e Humanas, Universidade Federal do ABC, Santo André, SP, 09210-170 Brazil

² B. I. Stepanov Institute of Physics, National Academy of Science of Belarus, Nezavisimosti Avenue 68, Minsk 220072, Belarus

³ BK21 Frontier Physics Research Division, Seoul National University, 08826 Seoul, South Korea

⁴ Department of Optics, Palacký University, 17. listopadu 12, 77146 Olomouc, Czech Republic

⁵ Department Physik, Universität Paderborn, Warburger Straße 100, 33098 Paderborn, Germany

⁶ Max-Planck-Institut für die Physik des Lichts, Staudtstraße 2, 91058 Erlangen, Germany

⁷ Departamento de Óptica, Facultad de Física, Universidad Complutense, 28040 Madrid, Spain

Abstract. The physical nature of any quantum source guarantees the existence of an effective Hilbert space of finite dimension, the physical sector, in which its state is completely characterized with arbitrarily high accuracy. The extraction of this sector is essential for state tomography. We show that the physical sector of a state, defined in some pre-chosen basis, can be systematically retrieved with a procedure using only data collected from a set of commuting quantum measurement outcomes, with no other assumptions about the source. We demonstrate the versatility and efficiency of the physical-sector extraction by applying it to simulated and experimental data for quantum light sources, as well as quantum systems of finite dimensions.

PACS numbers: 03.65.Ud, 03.65.Wj, 03.67.-a

Submitted to: *New J. Phys.*

1. Introduction

The physical laws of quantum mechanics ensure that all experimental observations can be described in an *effective* Hilbert space of finite dimension, to which we shall refer as the *physical sector* of the state. The systematic extraction of this physical sector is crucial for reliable quantum state tomography.

Photonic sources constitute an archetypical example where such an extraction is indispensable. Theoretically, the states describing these sources reside in an infinite-dimensional Hilbert space. Nonetheless, the elements of the associated density matrices decay to zero for sufficiently large photon numbers, so that there always exists a finite-dimensional physical sector that contains the state with sufficient accuracy. Reliable state tomography can thus be performed once this physical sector is correctly extracted.

Experiments on estimates of the correct physical sector have been carried out [1, 2]. One common strategy is to make an educated guess about the state (such as Gaussianity [3])

or rank-deficiency for compressed sensing [4–10]), which defines a truncated reconstruction subspace. For instance, in compressed sensing the rank of the state is assumed to be no larger than a certain value r , so that specialized rank- r compressed-sensing measurements can be employed to uniquely characterize the state with much fewer measurement settings. Very generally, educated guesses of certain properties of the state requires additional physical verifications. Algorithms for statistical model selection, such as the Akaike [11–13] or Schwarz criteria [14, 15] or the likelihood sieve [16, 17], have also been developed to estimate the physical sector. These algorithms provide another practical solution to reducing the complexity of the tomography problem. In the presence of the positivity constraint [18, 19], their application to quantum states becomes more sophisticated, as the procedures for deriving stopping criteria that supplies the final appropriate model subspace for the unknown state are intricate.

On the other hand, finite-dimensional systems represent another example for which a systematic physical-sector extraction becomes important. In the context of quantum information, ongoing developments in dimension-witness testing [20–24] offer some solutions to finding the minimal dimension of a black box required to justify the given set of measurement data in a device-independent way. Searching for dimension witnesses of arbitrary dimensions is still challenging [23].

In reference [25], we showed that, when the measurement device is calibrated, one can systematically extract the physical sector (that is, both the Hilbert-space support and dimension) and simultaneously reconstruct any unknown state directly from the measurement data without any assumption about the state. In this paper, we introduce an even more efficient procedure that extracts the physical sector of any state from the data without state reconstruction and provide the pseudocode. This procedure requires nothing more than data obtained from a set of commuting measurements. As in [25], the extraction of the physical sector does not depend on any other assumptions or calibration details about the source. By construction, this procedure has a linear complexity in the dimension of the physical sector. To showcase its versatility, we apply it to simulated and experimental data for photonic sources and systems of finite dimensions. In this way, we offer a deterministic solution to the problem of extracting the correct physical sector for any quantum state in measurement-calibrated situations.

2. Physical sectors and commuting measurements

2.1. What are physical sectors?

The concept of physical sectors and their relations to commuting measurements is probably best understood with a concrete example. Let us consider, in the Fock basis, a quantum state of light described by the density operator

$$\rho \hat{=} \begin{pmatrix} 0.9922 & * & 0.0877 & * & \cdots \\ * & * & * & * & \cdots \\ 0.0877 & * & 0.0078 & * & \cdots \\ * & * & * & * & \cdots \\ \vdots & \vdots & \vdots & \vdots & \ddots \end{pmatrix}, \quad (2.1)$$

where $*$ denotes elements of its density matrix that are so tiny that treating them to be zero incurs very small truncation errors. If all $*$ = 0, ρ is the pure state $|\rangle\langle|$ described by $|\rangle \propto |\alpha\rangle + |-\alpha\rangle$, with the coherent state of amplitude $\alpha = 0.3536$. The density matrix elements drops to zero for sufficiently large photon numbers as those of any physical state.

Some statistical reasoning for understanding the truncation error is in order. For now, we note that since all other $*$ elements are tiny, the state ρ is essentially fully characterized by a 3-dimensional sector, such that elements beyond this sector supply almost no contribution to ρ . This forms a truncated Hilbert subspace where tomography can be carried out reliably. This subspace is given by $\mathcal{H}_{\text{sub}} = \text{span}\{|0\rangle, |1\rangle, |2\rangle\}$. However from (2.1), we realize that this subspace is not the smallest one that supports ρ . The *smallest* subspace $\mathcal{H}_{\text{phys}} = \text{span}\{|0\rangle, |2\rangle\}$ is in fact spanned by only two basis kets. This defines the 2-dimensional *physical sector*.

In general, the physical sector $\mathcal{H}_{\text{phys}}$ is defined to be the *smallest Hilbert subspace* that fully supports a given state with a truncation error smaller than some tiny ε in some basis. Evidently, the choice of basis affects the description of $\mathcal{H}_{\text{phys}}$. If one already knows that ρ is close to $|\rangle\langle|$, then choosing $|\rangle$ as part of a basis gives a 1-dimensional $\mathcal{H}_{\text{phys}}$. Such knowledge is of course absent when ρ is unknown. In such a practical scenario in quantum optics, we may adopt the most common Fock basis for representing ρ and $\mathcal{H}_{\text{phys}}$. When dealing with general quantum systems, the basis that is most natural in typical experiments may be chosen, such as the Pauli computational basis for qubit systems.

2.2. How are physical sectors related to commuting measurements?

Let us revisit the example in (2.1). Because of the positivity constraint imposed on ρ , whenever a diagonal element is $*$, then elements in the row and column that intersect this element are all $*$. Also, if a diagonal element is not $*$, then it is obvious that $\mathcal{H}_{\text{phys}}$ is spanned by the basis ket for this diagonal element. For this example, the 2-dimensional $\mathcal{H}_{\text{phys}}$ completely characterizes ρ with the $2^2 = 4$ elements $\rho_{00}, \rho_{22}, \text{Re}(\rho_{02})$ and $\text{Im}(\rho_{02})$.

It follows that knowing the location of *significant* diagonal elements are all we need to ascertain $\mathcal{H}_{\text{phys}}$. For this purpose the only necessary tool is a set of *commuting* measurement outcomes with their common eigenbasis being the pre-chosen basis for $\mathcal{H}_{\text{phys}}$. After the measurement data are performed with these commuting outcomes, all one needs to do is perform an extraction procedure on the data to obtain $\mathcal{H}_{\text{phys}}$. This procedure would proceed to test a growing set of basis kets until it informs that the current set spans $\mathcal{H}_{\text{phys}}$ that fully supports the data. We note here that the extraction works for any other sort of generalized measurements in principle, although we shall consider commuting measurements in subsequent discussions since they are the simplest kind necessary for extracting physical sectors in large Hilbert-space dimensions.

3. The extraction of the physical sector

In some pre-chosen basis, the physical-sector extraction procedure (PSEP) iteratively checks whether its data are supported by the cumulative sequence of \mathcal{H}_{sub} with truncation error smaller than some tiny ε . PSEP starts deciding whether, say, $\mathcal{H}_{\text{sub}} = \text{span}\{|n_1\rangle, |n_2\rangle\}$ of the smallest dimension $d = 2$ adequately supports the data. If yes, it takes this as the 2-dimensional $\mathcal{H}_{\text{phys}}$. Otherwise, PSEP continues and decides if $\mathcal{H}_{\text{sub}} = \text{span}\{|n_1\rangle, |n_2\rangle, |n_3\rangle\}$ adequately supports the data, and so on until finally PSEP assigns a d_{phys} -dimensional $\mathcal{H}_{\text{sub}} = \mathcal{H}_{\text{phys}}$ with some statistical reliability. In each iterative step, there are three objectives to be met:

- (Ci) PSEP must decide if the data are supported with \mathcal{H}_{sub} spanned by some set of basis kets or not.
- (Cii) PSEP must report the reliability of the statement “ \mathcal{H}_{sub} supports ρ with truncation error less than ε ”.

- (Ciii) PSEP must ensure that the final accepted set of basis kets span $\mathcal{H}_{\text{phys}}$, the *smallest* \mathcal{H}_{sub} that supports ρ .

In what follows, we show that all these objectives can be fulfilled with only the information encoded in the measurement data.

3.1. Deciding whether the data are supported with some subspace

We proceed by first listing a few notations. In an experiment, a set of measured commuting outcomes are described by positive operators $\sum_j \Pi_j = 1$. They give measurement probabilities $p_j = \text{tr}(\rho \Pi_j)$ according to the Born rule. Each commuting outcome, in the common eigenstates $|n\rangle \langle n|$ that are also used to represent the physical sector, can be written as

$$\Pi_j = \sum_l c_{jl} |l\rangle \langle l| \quad (3.1)$$

with positive weights c_{jl} that characterize the outcome.

To decide whether the p_j s are supported with some Hilbert subspace \mathcal{H}_{sub} , the easiest way is to introduce Hermitian *decision observables*

$$W_{\text{sub}} = \sum_j y_j \Pi_j \quad (3.2)$$

for real parameters y_j . The decision observable for testing \mathcal{H}_{sub} , along with its y_j s, satisfies the defining property,

$$\langle n | W_{\text{sub}} | n \rangle = \begin{cases} 0 & \text{if } |n\rangle \in \mathcal{H}_{\text{sub}}, \\ a_n > 0 & \text{otherwise.} \end{cases} \quad (3.3)$$

This property automatically ensures that if ρ is *completely* supported in \mathcal{H}_{sub} , then the expectation value $\langle W_{\text{sub}} \rangle = \sum_j y_j p_j = 0$ with zero truncation error and PSEP takes this to be the physical sector ($\mathcal{H}_{\text{sub}} = \mathcal{H}_{\text{phys}}$). Quantum systems of finite dimensions possess states of this kind. In quantum optics however, ρ is not completely supported in any subspace, but possesses decaying density-matrix elements with increasing photon numbers [such as the example in (2.1)]. A laser source, for instance, cannot produce light of an infinite intensity. Furthermore, the Born probabilities p_j are never measured. Instead, the data consist of relative frequencies f_j that estimate the probabilities with statistical fluctuation. Therefore, if we define the decision random variable (RV)

$$w_{\text{sub}} = \sum_j y_j f_j \quad (3.4)$$

that estimates $\langle W_{\text{sub}} \rangle$, then PSEP may assign $\mathcal{H}_{\text{sub}} = \mathcal{H}_{\text{phys}}$ with a truncation error defined by $|w_{\text{sub}}|$ that is smaller than ε .

3.2. Quantifying the reliability of the truncation error report

The decision RV w_{sub} is an unbiased RV in that the data average of w_{sub} is the true value $\langle W_{\text{sub}} \rangle$ that PSEP achieves to estimate ($\mathbb{E}[w_{\text{sub}}] = \langle W_{\text{sub}} \rangle$). This means that in the limit of large number of measured detection events N for the data $\{f_j\}$, w_{sub} approaches its expected value $\mathbb{E}[w_{\text{sub}}]$, which in turn tends to zero in the limit $\mathcal{H}_{\text{sub}} \rightarrow \mathcal{H}_{\text{phys}}$. This limiting behavior invites us to understand the truncation error $|w_{\text{sub}}|$ using the well-known Hoeffding inequality [26], which states that

$$\alpha \equiv \Pr \{|w_{\text{sub}}| \geq \varepsilon\} \leq 2 \exp\left(-\frac{N\varepsilon^2}{2\sum_j y_j^2}\right). \quad (3.5)$$

This concentration inequality directly bounds the probability α of having a truncation error greater than or equal to ε , which is the significance level of the hypothesis that $w_{\text{sub}} = \mathbb{E}[w_{\text{sub}}]$ for all conceivable future data [27]. With

$$N \geq -\frac{2\ln(\alpha/2)}{\varepsilon^2} \sum_j y_j^2, \quad (3.6)$$

we are assured with α significance that the main factor for a nonzero $|w_{\text{sub}}|$ comes from insufficient support from \mathcal{H}_{sub} since statistical fluctuation is heavily suppressed.

One can obtain the more experimentally-friendly inequality [26]

$$\alpha \leq B_{\text{sub}} = 2 \exp\left(-\frac{|w_{\text{sub}}|^2}{2\Delta^2}\right) \quad (3.7)$$

in terms of the variance Δ^2 of w_{sub} , where we take $\varepsilon \approx |w_{\text{sub}}|$ as a sensible guide to the truncation-error threshold. For $N \gg 1$, the $1/N$ scaling of Δ^2 allows the quantity B_{sub} to provide an indication on the reliability of the statement “ \mathcal{H}_{sub} supports ρ with truncation error less than ε ” with a reasonable statistical estimate for Δ^2 from the data. If (3.7) holds for \mathcal{H}_{sub} and some pre-chosen α , then the assignment $\mathcal{H}_{\text{phys}} = \mathcal{H}_{\text{sub}}$ is made. Quite generally, w_{sub} and Δ^2 reveal the influence of both statistical and systematic errors [28]. Therefore, by construction, for sufficiently large N , \mathcal{H}_{sub} eventually converges to the unique $\mathcal{H}_{\text{phys}}$ at α significance with increasing size of the basis set for properly chosen \mathcal{H}_{sub} . The choice of \mathcal{H}_{sub} at each iterative step of PSEP must be made so that the final extracted support is indeed $\mathcal{H}_{\text{phys}}$, the smallest support for ρ .

3.3. Ensuring that the physical sector is extracted, not another larger support

To ensure that $\mathcal{H}_{\text{phys}}$ is really extracted, and not some other larger \mathcal{H}_{sub} that also supports the data, we once more return to the example in (2.1). For that pure state, in the Fock basis, the \mathcal{H}_{sub} that supports the state is effectively 3-dimensional, whereas $\mathcal{H}_{\text{phys}}$ is effectively 2 dimensional. With sufficiently large number of detection events N , if one naively carries out PSEP starting from $\mathcal{H}_{\text{sub}} = \text{span}\{|0\rangle\}$, PSEP would recognize that \mathcal{H}_{sub} cannot support the data, continue to test the next larger subspace $\mathcal{H}_{\text{sub}} = \text{span}\{|0\rangle, |1\rangle\}$, where it would again conclude insufficient support. Only after the third step will PSEP accept $\mathcal{H}_{\text{sub}} = \text{span}\{|0\rangle, |1\rangle, |2\rangle\}$ as the support at some fixed α significance. However, $\mathcal{H}_{\text{sub}} \neq \mathcal{H}_{\text{phys}}$.

In order to efficiently extract $\mathcal{H}_{\text{phys}}$, we need only one additional clue *from the data*, that is the relative size of the diagonal elements of ρ . We emphasize here that we are *not* interested in the precise values of the diagonal elements, but only a very rough estimate of their relative ratios to guide PSEP. With this clue, we can then apply PSEP using the appropriately ordered sequence of basis kets to most efficiently terminate PSEP and obtain the smallest possible support for the data. For the pure-state example, the decreasing magnitude of the diagonal elements gives the order $\{|0\rangle, |2\rangle\}$. For any arbitrary set of commuting Π_{j_s} , given the measurement matrix C of coefficients c_{jl} , sorting the column $C^{-}\mathbf{f}$, defined by the Moore-Penrose pseudoinverse C^{-} of C , in descending order suffices to guide PSEP \ddagger . This sorting permits the efficient completion of PSEP in $O(d_{\text{phys}})$ steps without doing quantum tomography. Other sorting algorithms are, of course, possible without any information about the diagonal-element estimates. One can perform other tests on different permutations of basis kets within the extracted Hilbert-subspace support, although the number of steps required to complete PSEP would be larger than $O(d_{\text{phys}})$.

\ddagger This is *not* tomography for the photon number distribution, but merely a very rough estimate on the relative ratios of diagonal elements, since $C^{-}\mathbf{f}$ is not positive.

3.4. An important afterword on physical-sector extraction

An astute reader would have already noticed that it is the $\mathcal{H}_{\text{phys}}$ within the field-of-view (FOV) of the data that can be reliably extracted. The FOV is affected by three factors: the degree of linear independence of the measured outcomes, the choice of some very large subspace to apply PSEP whose dimension does not exceed this degree of linear independence, and the accuracy of the data (the value of N). In real experiments, the number of linearly independent outcomes measured is always finite. With the corresponding finite data set, there exists a large subspace for extracting $\mathcal{H}_{\text{phys}}$, in which the decision observables W_{sub} always satisfy (3.3) for any \mathcal{H}_{sub} . For sufficiently large N , the collected data will capture all significant features of $\mathcal{H}_{\text{phys}}$ within this data FOV.

Indeed, if the source is *truly* a black box, then defining the data FOV can be tricky. True black boxes are, however, atypical in a practical tomography experiment since it is usually the observer who prepares the state of the source and can therefore be confident that the state prepared should not deviate too far from the target state as long as the setup is reasonably well-controlled. The data FOV should therefore be guided by this common sense. On the other hand, the extraction of $\mathcal{H}_{\text{phys}}$ in device-independent cryptography, where both the source and measurement are completely untrusted for arbitrary quantum systems, is still an open problem.

We note here that the measurement in (3.1) may incorporate realistic imperfections, such as noise, finite detection efficiency, that are faced in a number of realistic schemes. For instance, the commuting diagonal outcomes may represent on/off detectors of varying efficiencies, or incorporate thermal noise [29, 30]. All such measurements are presumed to be calibratable, as non-calibrated measurements require other methods to probe the source. As an example, suppose that the measurement is inefficient but still trustworthy enough for the observer to describe its outcomes by the set $\{\eta_j \Pi_j\}$ with unknown inefficiencies $\eta_j < 1$ that are simple functions of a few practical parameters of the setup such as transmissivities, losses and so forth. In other words, we have $\eta_j = \eta_j(T_1, \dots, T_l)$ for l that is typically much less than the total number of outcomes in practical experiments. Then the straightforward practice is to first calibrate all T_j s before using them to subsequently carry out PSEP for other sources. One may also choose to calibrate T_j already during the sorting stage by “solving” the linear system $\mathbf{t} = \mathbf{C}^{-1} \mathbf{f}'$, where $f'_j = f_j / \eta_j$ is now linear in the data f_j and nonlinear in T_j . The estimation of T_j falls under parameter tomography that is beyond the scope of this discussion, which focuses on the idea of locating physical sectors and not the exact values of density matrices.

4. The pseudocode for physical-sector extraction

Suppose we have a set of commuting measurement data $\{f_j\}$ that form the column \mathbf{f} , as well as the associated outcomes Π_j of some eigenbasis $\{|0\rangle, |1\rangle, |2\rangle, \dots\}$ that is adopted to represent $\mathcal{H}_{\text{phys}}$. For some pre-chosen basis and α significance, the pseudocode for PSEP is presented as follows:

STEP 1. Compute the measurement matrix \mathbf{C} and sort $\mathbf{C}^{-1} \mathbf{f}$ in descending order to obtain the ordered index i . Then, define the ordered sequence of basis kets $\{|n_{i_1}\rangle, |n_{i_2}\rangle, |n_{i_3}\rangle, \dots\}$.

STEP 2. Set $k = 0$ and $\mathcal{H}_{\text{sub}} = \text{span}\{|n_{i_1}\rangle\}$.

STEP 3. Construct W_{sub} by solving the linear system of equations in equation (3.3) for the y_j s.

STEP 4. Compute w_{sub} , Δ^2 and hence B_{sub} . For typical multinomial data, $\Delta^2 = \sum_{jk} y_j y_k (\delta_{j,k} p_j - p_j p_k) / N$.

STEP 5. Increase k by one and include $|n_{i_k}\rangle$ in \mathcal{H}_{sub} .

STEP 6. Repeat STEP 3 through 5 until $B_{\text{sub}} \geq \alpha$. Finally, report $\mathcal{H}_{\text{phys}} = \mathcal{H}_{\text{sub}}$ and α and proceed to perform quantum-state tomography in $\mathcal{H}_{\text{phys}}$.

5. Results

5.1. Quantum light sources

To illustrate PSEP, we consider the state in (2.1) and $\rho = |4\rangle \frac{1}{4} \langle 4| + |9\rangle \frac{1}{2} \langle 9| + |23\rangle \frac{1}{4} \langle 23|$. Simulated data are generated with a random set of commuting measurement outcomes. The extracted physical sectors are shown in figure 1.

Data statistical fluctuation may be further minimized by averaging B_{sub} over many different sets of commuting outcomes. Moreover, one can detect additional systematic errors that are not attributed to truncation artifacts by inspecting the corresponding histograms for errors larger than the statistical fluctuation.

We next proceed to experimentally validate PSEP by measuring photon-click events of a time-multiplexed detector (TMD). We use a fiber-integrated setup to generate and measure a mixture of coherent states, as depicted in figure 2(a). Coherent states are produced by a pulsed diode laser with 35 ps pulses at 200 kHz and a wavelength of 1550 nm. These pulses are then modulated with a telecom Mach-Zehnder amplitude modulator, driven with a square-wave signal at 230 kHz. This produces pseudorandom pulse patterns with two fixed amplitudes. After passing through fiber-attenuators, the state is measured with an eight-bin TMD [31, 32] with a bin separation of 125 ns and two superconducting nanowire detectors. We record statistics of all possible 2^8 bin configurations, which corresponds to a total of 256

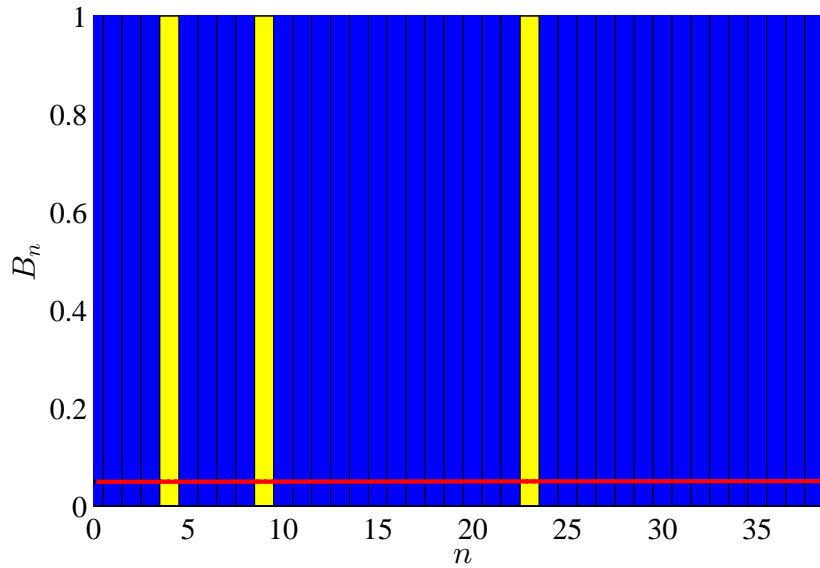


Figure 1. Physical sectors extracted with PSEP from simulated data of $N = 10^9$ detection events for (a) the pure state in (2.1) (black solid curve represents its photon-number distribution) and (b) the mixed state $\rho = |4\rangle \frac{1}{4} \langle 4| + |9\rangle \frac{1}{2} \langle 9| + |23\rangle \frac{1}{4} \langle 23|$. 2000 random sets of 40 commuting measurement outcomes were used to calculate the average B_{sub} in every iterative step k . The (blue) histogram plots B_{sub} for the default ordering of the basis kets labeled with $n = 0, 1, 2, \dots$. The physical sector $\mathcal{H}_{\text{phys}}$ (yellow region) is revealed after completing PSEP with respect to a 5% significance level ($\alpha = 0.05$) (red solid line).

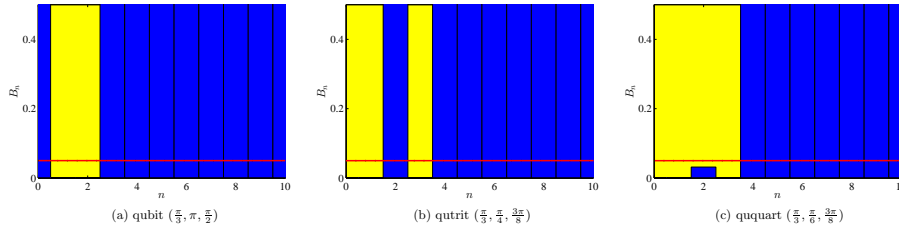


Figure 2. Schematic diagram of (a) the experimental setup to measure a mixture of coherent states and (b) the result of PSEP on the data for a mixture of two coherent states of mean photon numbers 9.043 and 36. Panel (a) describes coherent states from a pulsed laser pass through an amplitude modulator (AM), which switches between two values of attenuation. Neutral density (ND) filters further attenuate the light to the single photon level. The time multiplexing detector (TMD) consists of three fiber couplers, delay lines and superconducting nanowire single photon detectors (SPD). The physical sector in panel (b) is extracted from data of $N = 9.6 \times 10^6$ detection events. 5000 different sets of 60 outcomes out of the measured 256 were used to calculate the average B_{sub} in every iterative step. Other figure specifications follow those of figure 1.

TMD outcomes.

To characterize the TMD outcomes for the measurement, we perform standard detector tomography, using well calibrated coherent probe states [33, 34]. The setup is similar to the previous one, but we replace the modulator by a controllable variable attenuator. We calibrate the attenuator with respect to a power meter at the laser output. This allows us to produce a set of 150 probe states with a power separation of 0.2 dB.

TMD data of a statistical mixture of two coherent states are collected and PSEP is subsequently performed on these data. The accuracy of the extracted physical sector is ultimately sensitive to experimental imperfections. In this case, these imperfections are minimized owing to the state-of-the-art superconductor technology, the fruit of which is a histogram that is as clean as it gets in an experimental setting. Figure 2(b) provides convincing evidence of the feasibility and practical performance of the technique, where real data statistical fluctuation is present. This physical sector may subsequently be taken as the objective starting point for a more detailed investigation of the quantum signal with tools for tomography and diagnostics.

5.2. Finite-dimensional quantum systems

To analyze another aspect of PSEP, in this section, we apply it to quantum systems of finite dimensions with discrete-variable commuting measurement outcomes. As a specific example, we consider the arrangement in reference [22], which uses single photons to encode the information simultaneously in horizontal (H) and vertical (V) polarizations, and in two spatial modes (a and b). We define four basis states: $|0\rangle \equiv |H, a\rangle$, $|1\rangle \equiv |V, a\rangle$, $|2\rangle \equiv |H, b\rangle$, and $|3\rangle \equiv |V, b\rangle$. On passing through three suitably oriented half-wave plates at angles θ_1 , θ_2 , and θ_3 , the state of such hybrid systems can be converted to the pure state $\rho = |\theta_1, \theta_2, \theta_3\rangle \langle \theta_1, \theta_2, \theta_3|$, defined by

$$\begin{aligned} |\theta_1, \theta_2, \theta_3\rangle = & \sin(2\theta_1) \sin(2\theta_3) |0\rangle - \sin(2\theta_1) \cos(2\theta_3) |1\rangle \\ & + \cos(2\theta_1) \cos(2\theta_2) |2\rangle + \cos(2\theta_1) \sin(2\theta_2) |3\rangle. \end{aligned} \quad (5.1)$$

Thus, by adjusting the orientation angles of the wave plates, one could produce qubits, qutrits or ququarts from such a hybrid source. Here, we show that PSEP can rapidly extract $\mathcal{H}_{\text{phys}}$ by inspecting only the data measured from a set of commuting quantum measurements.

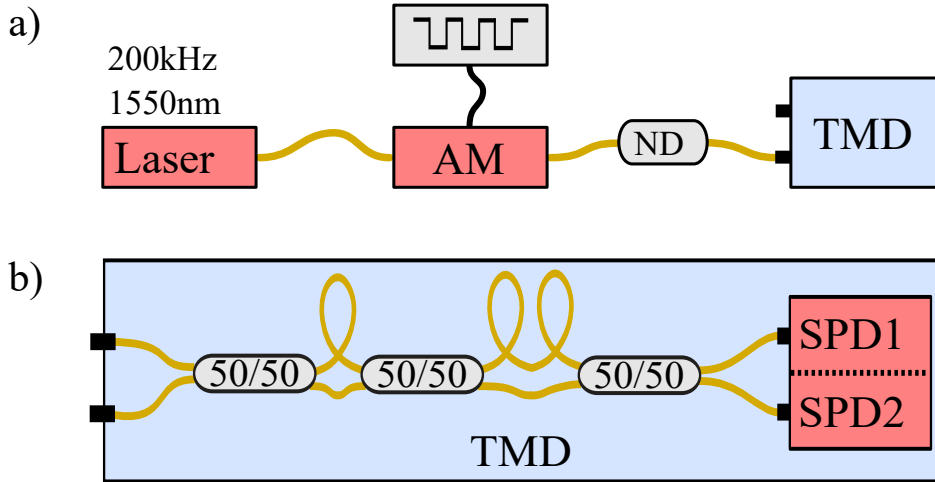


Figure 3. PSEP for hybrid quantum systems of finite dimensions that potentially generates either (a) a qubit state, (b) a qutrit state, (c) or a ququart state according to equation (5.1). With $N = 2.5 \times 10^6$ detection events, all three physical sectors (yellow region) are correctly extracted. For the ququart, the slightly higher reordered $B_{\mathcal{H}_{\text{sub}}}$ bar at $n = 2$ (which goes to zero for larger N) is a manifestation of the favorable sensitivity of the procedure to specific quantum-state features, not just the overall physical sector. Figure specifications follow those of figure 1.

Figure 3 presents the plots for a qubit, qutrit and ququart system characterized by the different $(\theta_1, \theta_2, \theta_3)$ configurations.

We have thus shown that in the typical experimental scenarios where the measurement setup is reasonably-well calibrated, and hence trusted, $\mathcal{H}_{\text{phys}}$ can be systematically extracted within the subspace spanned by the measurement outcomes. This allows an observer to later probe the details of the unknown but trusted quantum source using only the data at hand. Notice that the relevant basis states, labeled by n , form a basis for the commuting measurement on the black box. As such, this procedure is not a bootstrapping instruction. Rather, it systematically identifies the correct $\mathcal{H}_{\text{phys}}$ without any other *ad hoc* assertions about the source. In this way, we turn PSEP into an efficient *deterministic* dimension tester with complexity $O(d_{\text{phys}})$, as we have already learnt from section 3.3.

6. Conclusions

We have formulated a systematic procedure to extract the physical sector, the smallest Hilbert-subspace support, of an unknown quantum state using only the measurement data and nothing else. This is possible because information about the physical sector is always entirely encoded in the data. This extraction requires only few efficient iterative steps of the order of the physical-sector dimension.

We demonstrated the validity and versatility of the procedure with simulated and experimental data from quantum light sources, as well as finite-dimensional quantum systems. The results support the clear message that, for well-calibrated measurement devices, the physical sector can always be systematically extracted and verified with statistical tools, in which quantum-state tomography can be performed accurately. No *a priori* assumptions about the source, which require additional testing, are necessary. The proposed method should serve

as the reliable solution for realistic tomography experiments in quantum systems of complex degrees of freedom.

Acknowledgments

D. M. acknowledges support from the National Academy of Sciences of Belarus through the program “Convergence”, the European Commission through the SUPERTWIN project (Contract No. 686731), and by FAPESP (Grant No. 2014/21188-0). Y. S. T. acknowledges support from the BK21 Plus Program (Grant 21A2013111123) funded by the Ministry of Education (MOE, Korea) and National Research Foundation of Korea (NRF). J. Ř and Z. H. acknowledge support from the Grant Agency of the Czech Republic (Grant No. 15-03194S), and the IGA Project of Palacký University (Grant No. PRF 2016-005). J. T., R. K., G. H., and Ch. S. acknowledge the European Commission through the QCumber project (Contract No. 665148). Finally, L. L. S. S. acknowledges the Spanish MINECO (Grant FIS2015-67963-P).

- [1] Řeháček J and Paris M G A 2004 *Lecture Notes in Physics – Quantum State Estimation* vol 649 (Berlin Heidelberg: Springer)
- [2] Lvovsky A I and Raymer M G 2009 Continuous-variable optical quantum-state tomography *Rev. Mod. Phys.* **81** 299
- [3] Řeháček J, Olivares S, Mogilevtsev D, Hradil Z, Paris M G A, Fornaro S, D’Auria V, Porzio A and Solimeno S 2009 Effective method to estimate multidimensional Gaussian states *Phys. Rev. A* **79** 032111
- [4] Gross D, Liu Y K, Flammia S T, Becker S and Eisert J 2010 Quantum state tomography via compressed sensing *Phys. Rev. Lett.* **105** 150401
- [5] Cramer M, Plenio M B, Flammia S T, Somma R, Gross D, Bartlett S D, Landon-Cardinal O, Poulin D and Liu Y K, 2010 Efficient quantum state tomography *Nature Commun.* **1** 149
- [6] Flammia S T, Gross D, Liu Y K and Eisert J 2012 Quantum tomography via compressed sensing: error bounds, sample complexity and efficient estimators *New. J. Phys.* **14** 095022
- [7] Landon-Cardinal O and Poulin D 2012 Practical learning method for multi-scale entangled states *New. J. Phys.* **14** 085004
- [8] Baumgratz T, Gross D, Cramer M and Plenio M. B. 2013 Scalable reconstruction of density matrices *Phys. Rev. Lett.* **111** 020401
- [9] Riofrío C A, Gross D, Flammia S T, Monz T, Nigg D, Blatt R and Eisert J 2017 Experimental quantum compressed sensing for a seven-qubit system 2017 *Nature Comm.* **8** 15305
- [10] Steffens A, Riofrío C A, McCutcheon W, Roth I, Bell B A, McMillan A, Tame M S, Rarity J G and Eisert J 2017 *Quantum Sci. Technol.* **2** 025005
- [11] Akaike H 1974 A new look at the statistical model identification *IEEE T. Automat. Contr.* **19** 716
- [12] Usami K, Nambu Y, Tsuda Y, Matsumoto K and Nakamura K 2003 Accuracy of quantum-state estimation utilizing Akaike’s information criterion *Phys. Rev. A* **68** 022314
- [13] Yin J O S and van Enk S J 2011 Information criteria for efficient quantum state estimation *Phys. Rev. A* **83** 062110
- [14] Schwarz G 1978 Estimating the dimension of a model *Ann. Statist.* **6** 461
- [15] Guță M I, Kypraios T and Dryden I 2012 Rank-based model selection for multiple ions quantum tomography *New. J. Phys.* **14** 105002
- [16] Geman S and Hwang C-R 1982 Nonparametric maximum likelihood estimation by the method of sieves *Ann. Statist.* **10** 401
- [17] Artiles L M, Gill R D and Guță M I 2005 An invitation to quantum tomography *J. Roy. Stat. Soc. B* **67** 109
- [18] Anraku K 1999 An information criterion for parameters under a simple order restriction *Biometrika* **86** 141
- [19] Hughes A W and King M L 2003 Model selection using AIC in the presence of one-sided information *J. Statist. Plann. Inference* **115** 397
- [20] Brunner N, Pironio S, Acin A, Gisin N, Méthot A A and Scarani V 2008 Testing the dimension of Hilbert spaces *Phys. Rev. Lett.* **100** 210503
- [21] Hendrych M, Gallego R, Micuda M, Brunner N, Acin A and Torres J P 2012 Experimental estimation of the dimension of classical and quantum systems *Nat. Phys.* **8** 588
- [22] Ahrens J, Badziąg P, Cabello A and Bourennane M 2012 Experimental device-independent tests of classical and quantum dimensions *Nat. Phys.* **8** 592
- [23] Brunner N, Navascués M and Vértesi T 2013 Dimension witnesses and quantum state discrimination *Phys. Rev. Lett.* **110** 150501
- [24] Ahrens J, Badziąg P, Pawłowski M, Zukowski M and Bourennane M 2014 Experimental tests of classical and quantum dimensionality *Phys. Rev. Lett.* **112** 140401
- [25] Teo Y S, Mogilevtsev D, Mikhalychev A, Řeháček J and Z Hradil 2016 Crystallizing highly-likely subspaces that contain an unknown quantum state of light *Sci. Rep.* **6** 38123
- [26] Hoeffding W 1963 Probability inequalities for sums of bounded random variables *J. Amer. Statist. Assoc.* **58** 13
- [27] Mecatti F *et al* 2014 *Contributions to Sampling Statistics* (Cham Switzerland: Springer)
- [28] Mogilevtsev D, Hradil Z, Řeháček J and Shchesnovich V S 2013 Cross-validated tomography *Phys. Rev. Lett.* **111** 120403
- [29] Hradil Z, Mogilevtsev D, and Řeháček J, Biased tomography schemes: an objective approach *Phys. Rev. Lett.* 2006 **96**, 230401
- [30] Harder G, Mogilevtsev G, Korolkova N, Silberhorn C, *Phys. Rev. Lett.* 2014 **113** 070403
- [31] Achilles D, Silberhorn C, Śliwa C, Banaszek K and Walmsley I A 2003 Fiber-assisted detection with photon number resolution *Opt. Lett.* **28** 2387
- [32] Avenhaus M, Laiho K, Chekhova M V and Silberhorn C 2010 Accessing higher order correlations in quantum optical states by time multiplexing *Phys. Rev. Lett.* **104** 063602
- [33] Řeháček J, Mogilevtsev D and Hradil Z 2010 Operational tomography: Fitting of data patterns *Phys. Rev. Lett.* **105** 01040
- [34] Harder G, Silberhorn C, Řeháček J, Hradil Z, Motka L, Stoklasa B and Sánchez-Soto L L 2014 Time-multiplexed measurements of nonclassical light at telecom wavelengths *Phys. Rev. A* **90** 042105

